ELSEVIER

Marine Geology 180 (2002) 87–103

MARINE GEOLOGY
INTERNATIONAL JOURNAL OF MARINE GEOLOGY, GEOCHEMISTRY AND GEOPHYSICS

www.elsevier.com/locate/margeo

The late Miocene onset of high productivity in the Benguela Current upwelling system as part of a global pattern

Liselotte Diester-Haass [a,*], Philip A. Meyers [b], Laurence Vidal [c,1]

[a] *Zentrum für Umweltforschung der Universität, 66041 Saarbrücken, Germany*
[b] *Department of Geological Sciences, The University of Michigan, Ann Arbor, MI 48109-1063, USA*
[c] *Fachbereich Geowissenschaften der Universität Bremen, 28334 Bremen, Germany*

Received 1 July 2000; received in revised form 10 January 2001; accepted 25 May 2001

Abstract

We have examined the history of the elevated primary productivity associated with the Benguela Current upwelling system off southwest Africa using sediments from 7.5 to 4.8 Ma at Ocean Drilling Program Site 1085 in the middle Cape Basin. Sedimentation rates are low until 6.9 Ma. Low accumulation rates of benthic foraminifers and organic carbon indicate that biological productivity was also low. Paleoproductivity dramatically increased at 6.7–6.5 Ma and was highly variable until 4.8 Ma with productivity maxima during cooler periods. The presence of radiolarian opal only between 5.8 and 5.2 Ma suggests an interlude of silica-rich intermediate water in the Cape Basin. The onset of heightened productivity under the Benguela Current is mirrored by similar increases reported between 6.9 and 6.7 Ma in the tropical eastern Pacific, the western and northern Pacific, and the Indian Ocean. The similarity between the patterns at Site 1085 and in the Pacific and Indian Oceans suggests that the dramatic productivity increase off southwest Africa is part of a global response to paleoceanographic changes.

Keywords: late Miocene; export productivity; upwelling; $CaCO_3$ MAR; organic carbon MAR; benthic foraminiferal accumulation rates

1. Introduction

A major increase in marine biological productivity during the late Miocene–early Pliocene has been documented in widespread areas of the global ocean. Locations include upwelling areas in the equatorial Pacific and Indian Oceans, where dramatic increases in mass accumulation rates of opal, organic and inorganic carbon, phosphorus, and barium (Van Andel et al., 1975; Peterson et al., 1992; Berger et al., 1993; Farrell et al., 1995; Schroeder et al., 1997; Dickens and Owen, 1999) and expansion of the oxygen minimum zone (Dickens and Owen, 1999) have been noted between 7 and 6 Ma. Evidence of similar late Miocene increases in productivity has been described at high latitudes in the northwest Pacific (Rea et al., 1995) and subpolar South Atlantic Ocean (Froelich et al., 1991). The widespread occurrence

[1] Present address: CEREGE, Europôle de l'Arbois, BP 80, 13545 Aix en Provence, France.

* Corresponding author.
E-mail address: a.l.haass@t-online.de (L. Diester-Haass).

0025-3227/02/$ – see front matter
PII: S0025-3227(01)00207-9

of elevated marine productivity from about 7.0 Ma in the late Miocene to the early Pliocene has been dubbed the 'biogenic bloom' by Farrell et al. (1995).

The biogenic bloom appears during a period of major paleoclimatic and paleoceanographic changes. Ice caps expanded at both poles, the Isthmus of Panama gradually uplifted (Farrell et al., 1995), North Atlantic deep water (NADW) formation evolved and began to dominate global deep circulation (Farrell et al., 1995 and references therein), and isolation of the Mediterranean led to the 'Messinian salinity crisis' (Hodell et al., 1994; Krijgsman et al., 1999). However, it is not well understood how these global changes contributed to the causes and consequences of the bloom.

Information about the biogenic bloom comes mainly from upwelling areas in the equatorial Indian and Pacific Oceans. Information from coastal upwelling zones and from the Atlantic Ocean is sparse. We help to fill both these gaps by providing information about productivity changes during the late Miocene to early Pliocene (7.5–4.8 Ma) in the Benguela Current upwelling system off southwest Africa.

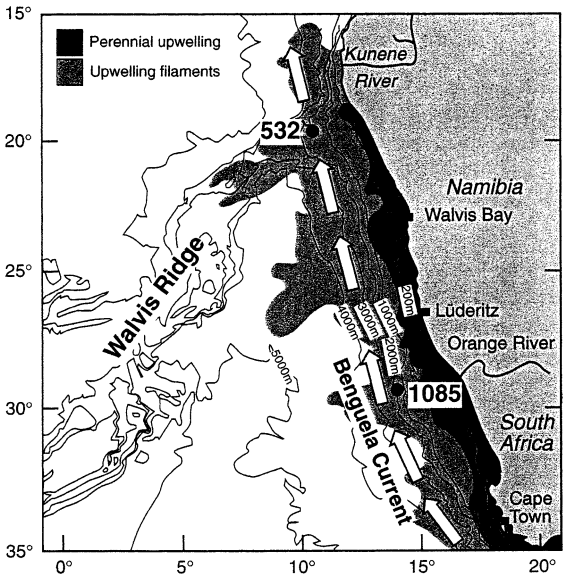

Fig. 1. Locations of ODP Site 1085 and DSDP Site 532 relative to the general axis of the Benguela Current (bold arrow). Areas of perennial and periodic upwelling as defined by Lutjeharms and Stockton (1987) are shown by shading.

2. Background

2.1. Benguela Current and elevated productivity

The combination of the northwest-flowing Benguela Current and SE trades is responsible for the 150–200 km wide upwelling zone on the continental shelf and at the shelf edge off southwest Africa (Fig. 1) (Stramma and Peterson, 1989). The current leaves its coast-parallel direction and turns more to the west at 23–20°S, where it meets warm tropical water masses flowing from the north. Eight upwelling cells occur along the southwest African margin between 15 and 35°S (Shannon and Pillar, 1986); the strongest is situated offshore of Lüderitz at 25°S. Nutrient-rich water upwells from about 200 m depth (Hart and Currie, 1960) and is derived from the South Atlantic central water mass. Productivity reaches values of up to 180 g/cm^2/yr (Berger, 1989). A signal of this near-coastal upwelling is carried offshore to the continental slope by west-flowing filaments of upwelled water, which can be up to 1000 km long and extend as far as 1300 km offshore (Summerhayes et al., 1995). Thermal fronts demarcate the seaward extent of upwelled water bodies (Shannon and Nelson, 1996).

The shelf edge upwelling is defined by high concentrations of nutrients and organisms. Here radiolaria and fishes flourish, whereas diatoms, which are very abundant in the nearshore upwelling zone, do not dominate shelf edge upwelling (Summerhayes et al., 1995). The African coast along the upwelling area is a dry desert area; the only perennial river is the Orange River, whose muds are transported south by prevailing bottom currents (Summerhayes et al., 1995).

2.2. Previous work

The Neogene and Quaternary history of the southwest African upwelling system was previously studied using cores collected by Deep Sea Drilling Project Legs 40 and 75 (Bolli et al., 1978;

Hay et al., 1984). Paleoceanographic reconstructions based on these sedimentary records have been limited by two problems: (1) interrupted core sequences because of drilling disturbances and spot coring, and (2) core sites distant from the main upwelling centers. Results from these two legs nonetheless yielded an important albeit preliminary history of the regional upwelling. Diester-Haass et al. (1990, 1992) hypothesized that the Benguela Current shifted progressively northwards since the middle Miocene to reach the Walvis Ridge and thereby to initiate upwelling at about 10.5 Ma (all ages are adjusted from the Berggren et al. (1985) time scale to the Berggren et al. (1995) time scale). From 10.5 Ma to 5.4 Ma, upwelling was stronger during glacial periods over Walvis Ridge, whereas in interglacial periods it was weaker because the Benguela Current turned to the west within the Cape Basin and did not reach the Walvis Ridge. Since 5.4 Ma, upwelling over the Walvis Ridge has been more intense during interglacial periods and weaker during glacial periods, a phenomenon that may be explained either by a northward shift of the Benguela Current into the Angola Basin (Diester-Haass et al., 1990, 1992) or by changes in global hydrography that led to nutrient-poor intermediate water off southwest Africa during glacial periods (Hay and Brock, 1992).

The preliminary reconstruction of the Benguela Current upwelling system suffers from poor temporal resolution and the fact that essentially all of the Miocene information comes from one location, Site 362/532, which is on the Walvis Ridge continental terrace (Fig. 1). Sediment records obtained during Ocean Drilling Program (ODP) Leg 175 provide a new opportunity to study the history of upwelling in continuous and relatively undisturbed sediment sequences from multiple locations along the southwest African margin with markedly improved temporal resolutions. As a first step in the overall paleoceanographic reconstruction of the Benguela Current system, we focus on the late Miocene sediment record at ODP Site 1085 in the Cape Basin using a time interval that spans the onset of elevated productivity on the Walvis Ridge (Siesser, 1980; Meyers et al., 1983).

3. Samples and analysis

3.1. Location and sampling

ODP Site 1085 (29°22.4465′S, 13°59.4064′E, 1713 m water depth) is located beneath the southern part of the Benguela Current upwelling region off the mouth of the Orange River (Fig. 1). Present-day upwelling above this location is highly seasonal with its maximum in the austral summer (Wefer et al., 1998).

We obtained 10 cm^3 samples at intervals of 50–100 cm from Cores 28H–33H and 34X–42X (251–392 m below sea floor (mbsf)) of Hole 1085A. The sampling intervals correspond to about one sample every 5–30 kyr. Additional samples were collected from Core 30H of Hole 1085B (270–279 mbsf) to fill a missing interval from 269 to 279 mbsf in Hole 1085A and thereby to create a continuous record. The entire sampling section consists predominantly of greenish-gray nannofossil-foraminifer oozes (Wefer et al., 1998).

3.2. Analytical strategies

Reconstruction of productivity in continental margin environments from individual parameters can be problematic because the signal of overlying productivity is often difficult to separate from material transported downslope from the shelf and because of dissolution of carbonate and siliceous microfossils. We therefore employed multiple parameters to reconstruct the paleoproductivity history at Site 1085. Accumulation rates of radiolaria (no diatoms were found) are usually related to productivity, although water mass chemistry can also affect their abundance (Summerhayes et al., 1995; Lange and Berger, 1993; Nelson et al., 1995). Benthic foraminiferal accumulation rates (BFAR) are considered to be a good proxy for export paleoproductivity (Herguera and Berger, 1991; Nees, 1997; Schmiedl and Mackensen, 1997; van der Zwaan et al., 1999). Because benthic foraminifers depend on food delivered from the photic zone, the amount and nutritional value of this export is therefore reflected in the abundance of these fauna. In addition, comparison of BFAR in two grain-size fractions (125–250

μm, 250–1000 μm) helps to distinguish between redeposited and in situ origins of these proxies.

Accumulation rates of echinoderms, which also depend mainly on organic matter supply from the photic zone (Gooday and Turley, 1990), are another proxy for paleoproductivity. Organic carbon concentrations and accumulation rates reflect paleoproductivity of overlying waters, but they also sometimes record lateral supply from shelf–shelf edge environments, which can increase during sea level lowstands (Diester-Haass et al., 1992; Sancetta et al., 1992).

Changes in the dissolution of carbonate microfossils can result from variations in paleoproductivity. Increased supply of organic matter from the photic zone enhances microbial activity and thus respiratory calcite dissolution (Archer and Maier-Reimer, 1994). This parameter, however, needs confirmation by other parameters to be interpreted in terms of productivity changes. We measured carbonate dissolution by well-established proxies, fragmentation of planktic foraminifers and benthic/planktic (B/P) ratios of foraminifers. Processes in addition to productivity may influence carbonate dissolution, oxygen content of bottom water, sedimentation rates, species assemblage, depth of burial, and even sample preparation. The existence of such factors mandates use of a multiproxy approach such as we employed.

The possible impact of carbonate dissolution on benthic foraminiferal shells, which are less sensitive to dissolution than planktic ones, is an untested problem in our study. However, the general lack of strong fragmentation of planktic foraminifera suggests that benthic numbers are not markedly affected by dissolution. Furthermore, we found that accumulation rates of benthic foraminifera increase when dissolution of planktic foraminifera increases. This observation gives us confidence that benthic foraminifera at Site 1085 are not markedly dissolved.

An important goal of our investigation is to relate productivity variations to global changes such as in ice volumes and sea level. Particles such as glauconite, phosphorite, relict shell material, and worn mollusc shells, all of which originate from the shelf (Rogers and Bremner, 1991), may indicate lowered sea level when found in sediments from the 1700 m depth of Site 1085. This change in composition and texture occurs because seaward migration of the shoreline during regressions increases downslope transfer of resuspended shelf sediments. In addition, changes in concentrations and grain-size distributions of quartz, mica and other clastic minerals may indicate variations in eolian and/or fluvial supply of continental sediment components.

3.3. Age control

Our chronostratigraphy at Site 1085 is based on a high-resolution benthic foram $\delta^{18}O$ record, which reflects a combination of deep water temperature changes and fluctuations in continental ice volume. Spectral analysis of the $\delta^{18}O$ results shows that orbital obliquity (41 kyr period) dominates the late Miocene record at Site 1085 (Vidal et al., 2002). Therefore, the cyclicity was extracted from the isotope record and tuned to obliquity for the time interval 7.1–4.8 Ma. Age control points were obtained for nearly every obliquity cycle for the time interval 6.5–4.8 Ma (Vidal et al., 2002). For the time interval 7.1–6.5 Ma, age control is on the order of two obliquity cycles because of the lower amplitude in $\delta^{18}O$ variations. Control points obtained for the entire time interval must be interpreted cautiously because of filtering errors due to the limited length (2.3 Myr) of the record.

Comparison of the benthic foram $\delta^{18}O$ chronostratigraphies of Site 1085 and of the deep Pacific ODP Site 846 (Shackleton et al., 1995) shows that the ages of the major isotopic events for the late Miocene agree well, thereby substantiating the isotopically tuned Site 1085 age model (Vidal et al., 2002). The Site 1085 chronostratigraphic interval was extended to 7.5 Ma by extrapolation to the calcareous nannofossil datum at 8.6 Ma (FO Discoaster quinqueceramus: Wefer et al., 1998, Table 1).

Linear sedimentation rates (LSRs) derived from the tuned age model and the rates based on shipboard biostratigraphy and paleomagnetic ages agree fairly well for the long-term trend (Fig. 2). The high-resolution chronostratigraphic control

Table 1
$\delta^{18}O$ control points and absolute ages based on calcareous nannofossil biostratigraphy of ODP Site 1085 from Wefer et al. (1998)

Core	mbsf	Age (ka)
27H	245	4.62
29H	265	4.8
31H	280	5.23
33H	300.89	5.54
36X	329.24	5.9
40X	367.94	6.6
41X	377.57	6.9
45X	415.82	8.6
47X	435.59	9.1

points were applied to the sedimentary records to calculate sediment mass accumulation rates (MARs).

3.4. Analytical procedures

2 g of each sample were set aside for carbon measurements, and the remainder was washed through 40 and 63 μm sieves. The <40 μm fraction was set aside for clay mineral analyses, whereas the >40 μm fraction was used for a combined coarse fraction and isotope analysis (this study and Vidal et al., 2002). The >63 μm fraction was sieved into 63–125, 125–250, 250–500, >500 μm fractions. In each fraction, 800 grains (if present) were counted and up to 25 different biogenous, terrigenous and authigenous components were separated. The percent composition of the sand and coarse silt (40–63 μm) fraction was calculated by multiplying the percentage of each individual component in each fraction by the weight of the fraction. These data form the basis for calculations of component mass accumulation rates (MARs) according to the equation:

$$MAR_{component} = (\%\ component/100 \times MAR_{bulk\ sediment}) \times 1000$$

where $MAR_{component}$ and $MAR_{bulk\ sediment}$ are given in mg/cm^2/kyr.

Freeze-dried samples of bulk sediment were analyzed for calcium carbonate concentrations using the carbonate bomb technique of Müller and Gastner (1971). The carbonate-free residue remaining after the carbonate bomb analysis was collected, rinsed, and dried. Amounts of organic carbon and nitrogen in the carbonate-free residues were measured with a Carlo Erba 1108 CHNS analyzer (Verardo et al., 1990). Total organic carbon (TOC) concentrations ($\pm 0.05\%$) were calculated on a whole-sediment basis, adjusting for the carbonate concentrations determined from the bomb technique. Organic C/total N ratios were calculated on an atomic basis.

Organic $\delta^{13}C$ measurements were conducted in the Stable Isotope Laboratory at The University of Michigan. The $^{13}C/^{12}C$ ratios of the oxidized organic carbon were determined with a Finnigan Delta S mass spectrometer calibrated with the NBS-21 (graphite) standard. Data are corrected for ^{17}O and are expressed in conventional $\delta^{13}C$ notation (± 0.1‰) relative to the PDB standard.

Determinations of the $\delta^{18}O$ values of shells of the benthic foraminifera *Cibicidoides wuellerstorfi* and *C. kullenbergi* in the >150 μm fraction samples were done at the Geosciences Department at Bremen University using a Finnigan MAT 252 mass spectrometer. Data are reported in permil versus PDB after calibration with NBS 19. The mean external reproducibility is ± 0.07‰.

4. Results

Linear sedimentation rates begin to increase stepwise at 6.9 Ma from 2 cm/kyr to reach as high as 12 cm/kyr at 5.3 Ma (Fig. 2, lower panel). This increase was preceded between 9.1 and 7.0 Ma by LSRs that remained below 5 cm/kyr. Similar increases have been documented in sedimentary records from the South Atlantic (Cepek et al., 1999) and are discussed in Vidal et al. (2002). Benthic $\delta^{18}O$ values (Fig. 2, upper panel) vary widely between 2.5 and 3.4‰. The amplitude of the $\delta^{18}O$ shifts increases at about 6.5 Ma from 0.25 to 0.5‰. We attribute the distinct maxima in $\delta^{18}O$ to glacial intervals and the minima to interglacial periods.

Analytical results for individual samples are available in Diester-Haass et al. (2001). We summarize these data, identify relations between the

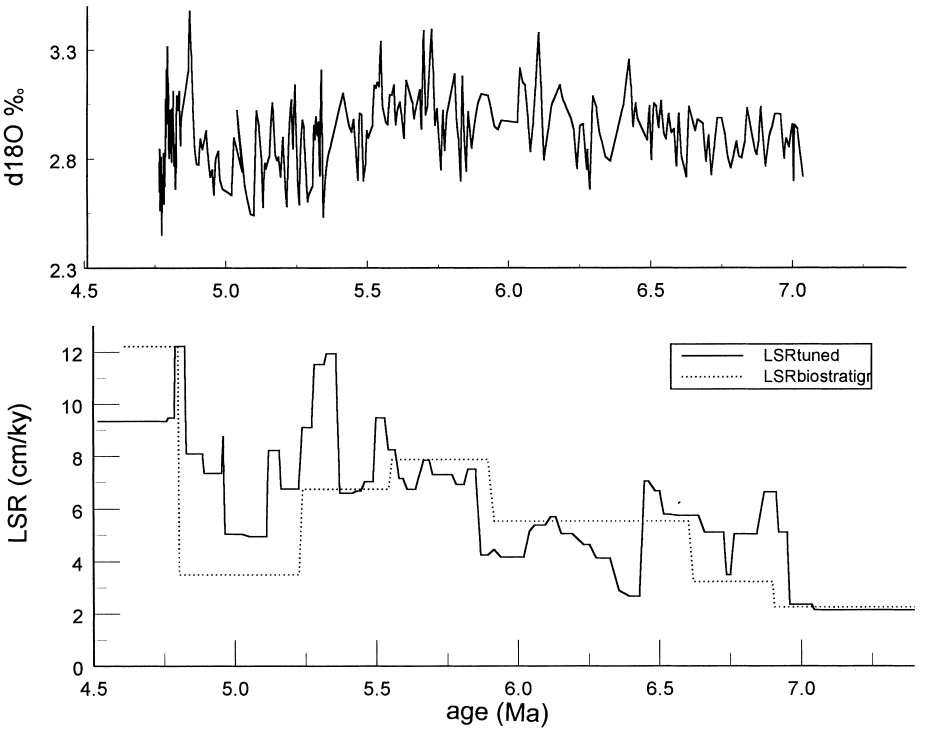

Fig. 2. Lower panel: Linear sedimentation rates (LSRs) at ODP Site 1085 in the Cape Basin based on biostratigraphic data from Wefer et al. (1998) and on benthic foram $\delta^{18}O$ measurements and refined by orbital tuning. Upper panel: Benthic foraminiferal (*C. wuellerstorfi* and *C. kullenbergi*) $\delta^{18}O$ values (‰ PDB) in ODP Site 1085 sediments.

multiple parameters that we determined, and describe changes that occurred over the 2.6 Myr period that we studied in the sections that follow.

The sand fraction constitutes $<2\%$ of the total sediment prior to 6.75 Ma and then increases up to 6% with high variability in younger portions of

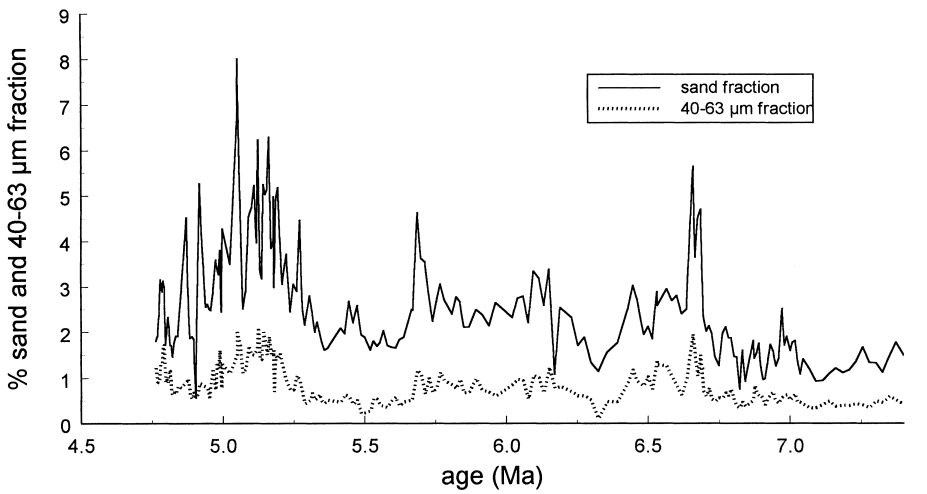

Fig. 3. Percentages of sand (>63 µm) and 40–63 µm fractions in total dry sediment at ODP Site 1085.

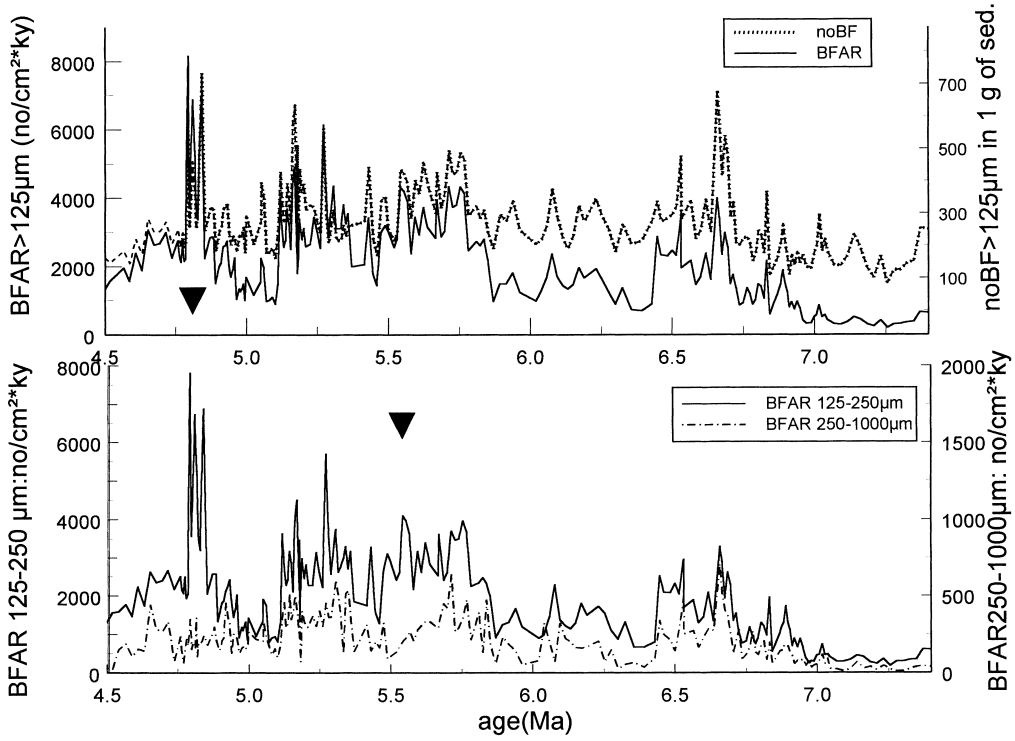

Fig. 4. Upper panel: Numbers of total benthic foraminifers >125 μm in 1 g of sediment and benthic foraminiferal accumulation rates (BFAR) in numbers per cm^2/kyr at ODP Site 1085. Lower panel: Numbers of 125–250 μm and 250–1000 μm sized benthic foraminifers per cm^2/kyr in sediment from ODP Site 1085.

the record (Fig. 3). The proportion of silt varies in parallel (Fig. 3). The remainder of the sediment is fine-grained (<40 μm) mud containing mainly nannofossils and terrigenous matter (Wefer et al., 1998).

The main components of the sand fraction are planktic (50–95%) and benthic foraminifers (5–30%) and pyrite crystals (0–20%). The concentration of benthic foraminifers >125 μm increases from <300/g in sediment deposited prior to 6.7 Ma to as high as 600–700/g in younger sediment (Fig. 4, upper panel). BFAR in the >125 μm fractions increase from <1000/cm^2/kyr prior to 6.7 Ma to peak at more than 7000/cm^2/kyr in early Pliocene intervals (Fig. 4, upper panel). BFAR in the 125–250 and 250–1000 μm size fractions vary in parallel and show the same trend as the >125 μm benthic foraminifers (Fig. 4, lower panel). Two exceptions, in which the BFAR of the 125–250 μm benthic foraminifers increase while those of the coarser ones decrease, are noted in Fig. 4, lower panel (indicated by triangles).

Radiolarian microfossils are found only in the period 5.8–5.25 Ma (Fig. 5). Their maxima coincide with low $\delta^{18}O$ values (i.e. warmer periods), except at 320 mbsf (5.7 Ma) when a high radiolarian accumulation rate occurs during a cold period (Fig. 2, upper panel and Fig. 5). Accumulation rates of echinoids increase in sediment deposited after 6 Ma (Fig. 5). Some of their maxima correspond to BFAR maxima (Fig. 5 and Fig. 4, upper panel).

Values of the two carbonate dissolution proxies, the B/P foraminiferal ratio and fragmentation of planktic foraminifers, are shown in Fig. 6. Small variations of both parameters are often simultaneous, although trends of absolute values sometimes diverge because fragmentation is influenced not only by dissolution but also by species assemblages. A major divergence occurs between

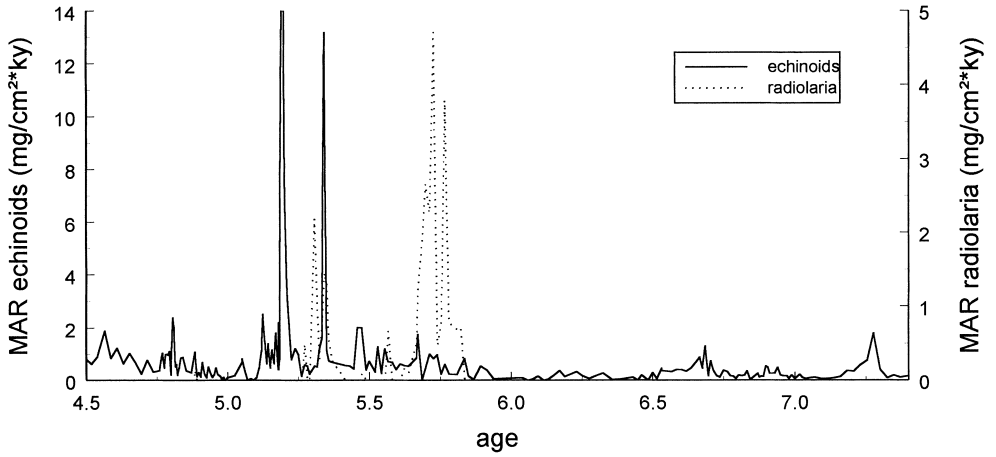

Fig. 5. Accumulation rates of radiolaria and echinoids in mg/cm^2/kyr in sediments from ODP Site 1085. No other opaline microfossils were found.

5.25 and 5.0 Ma, when fragmentation is high but B/P ratios are low.

$CaCO_3$ concentrations vary between 50 and 85% (Fig. 7, lower panel), and the $CaCO_3$ MAR (Fig. 7, upper panel) increases in the same three steps over time as seen in the BFAR (Fig. 4). Organic carbon percentages increase from $<1\%$ prior to 6.5 Ma to reach values as high as 2.5% in the younger section (Fig. 7). The MARs of organic carbon increase at 6.5 Ma and show cyclic variations parallel to those of $CaCO_3$ (Fig. 7, upper panel). Because of their setting offshore from a coastal desert, it is likely that the Site 1085 sediments contain mostly marine-derived organic matter (Wefer et al., 1998).

The percentage of terrigenous particles is low ($<0.5\%$) in the >63 μm fractions, but increases after 5.7 Ma. This contribution can be as great as 5% in the 40–63 μm fraction. Accumulation rates of terrigenous material are low prior to 5.7 Ma and have maxima at 5.6–5.3 Ma and at 4.8 Ma, when sand-sized terrigenous matter also increases

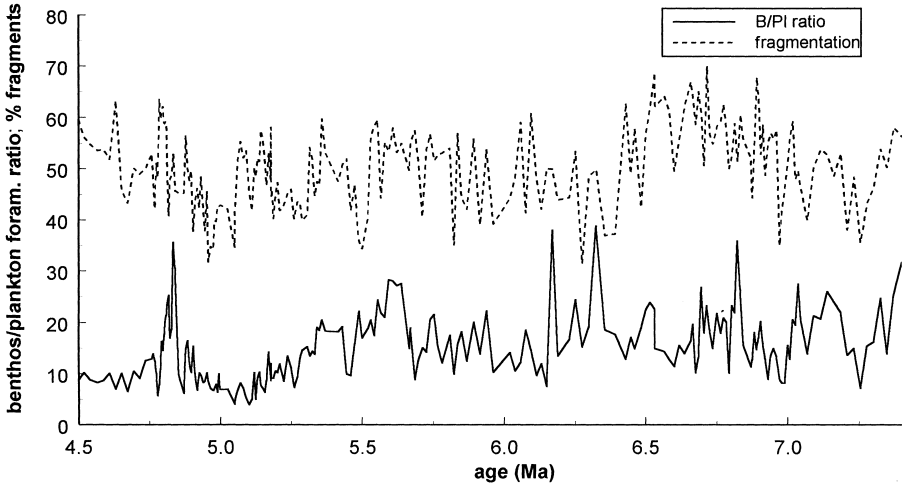

Fig. 6. Carbonate dissolution as indicated by means of benthic/planktic foraminiferal ratios and percent fragmentation of planktic foraminifers at ODP Site 1085 (for calculation see text).

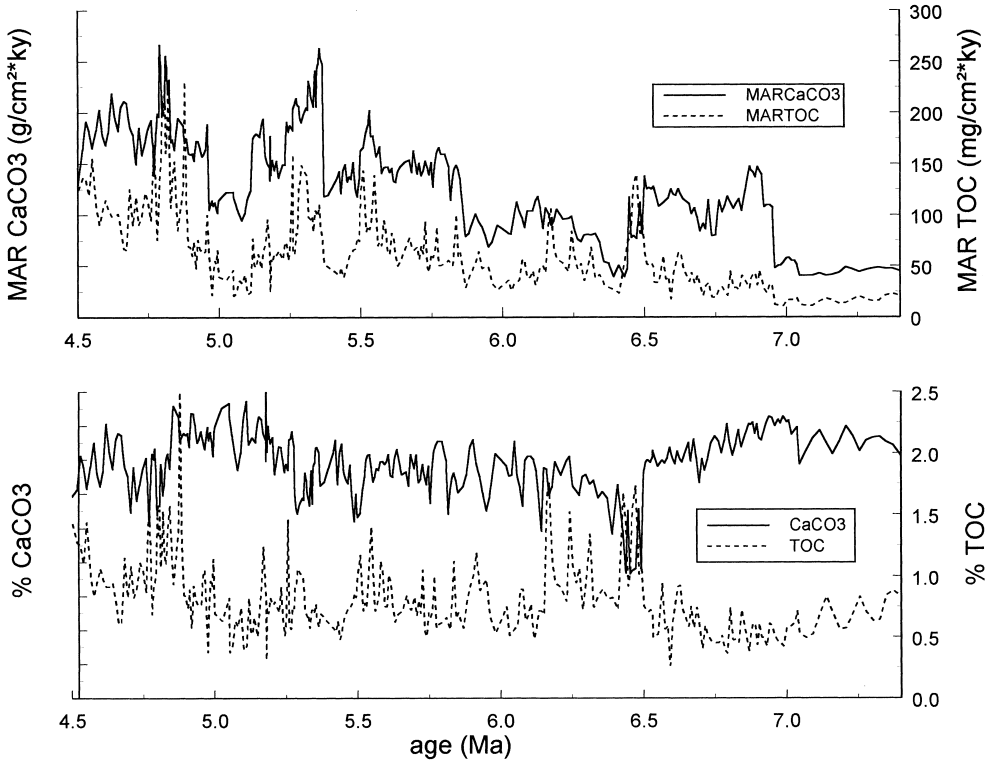

Fig. 7. Lower panel: Concentrations of $CaCO_3$ and organic carbon in weight percent dry sediment at ODP Site 1085. Upper panel: Accumulation rates of $CaCO_3$ and organic carbon in sediments from ODP Site 1085.

(Fig. 8, lower panel). The amount of glauconite (Fig. 8, upper panel), which is a proxy for downslope transport of shelf sediment (McRae, 1972), is temporally similar to contributions of terrigenous particles. This component has highest values and largest grain sizes at 4.75 Ma, which is coeval with maxima in both terrigenous matter and relict worn shell material.

5. Discussion

5.1. Late Miocene productivity evolution in the Cape Basin

Sedimentation patterns change dramatically at Site 1085 between 6.9 and 6.5 Ma. Linear sedimentation rates, sand and silt concentrations, and MARs of biogenous components simultaneously increase. In addition, the amplitudes of variations in sand concentrations are small prior to 6.7 Ma but increase afterwards.

Are these fundamental changes a consequence of changes in the amount of sediment winnowing, dissolution of carbonates, delivery of terrigenous particles, or marine production? Winnowing preferentially removes fine particles, so it could be responsible for an increase in percentage of coarse silt and sand. However, prior to 6.7 Ma, sand and coarse silt are at their lowest percentages. Winnowing is therefore not a plausible explanation for the low LSR before 6.9 Ma. Carbonate dissolution is also not a plausible explanation for the low LSR, because both dissolution proxies – fragmentation of planktic foraminifers and B/P ratios – are similar to times when the LSR is much higher. However, terrigenous input appears to have been low prior to about 6.5 Ma (Fig. 8, lower panel), and magnetic susceptibility values (Wefer et al., 1998) and iron contents (Vidal et al., 2002),

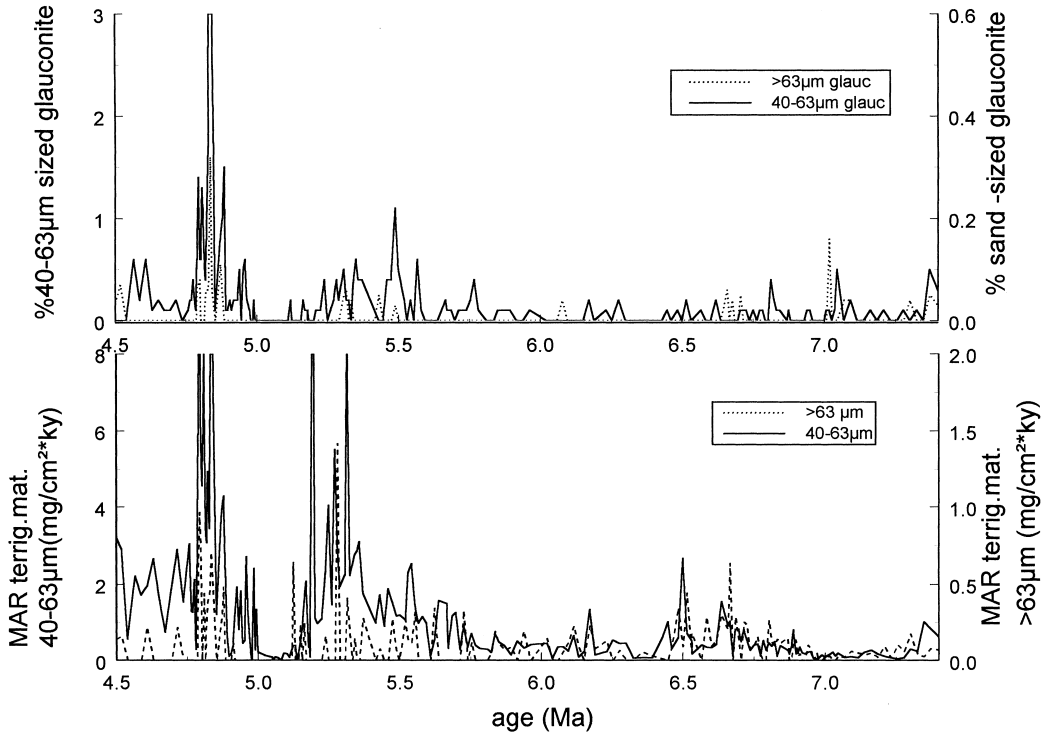

Fig. 8. Lower panel: Accumulation rates of terrigenous matter in the >63 and 40–63 µm fractions of sediment. Upper panel: Percentage of glauconite in >63 and 40–63 µm fractions.

which are both proxies of terrigenous sediment contributions, are at a minimum. The increase in LSR might therefore be at least partly due to an increase in terrigenous input.

A remaining possibility for the lower LSR is lower marine productivity prior to 6.7–6.5 Ma. Concentrations and accumulation rates of the sand fraction, benthic foraminifers, and organic carbon begin to increase stepwise after about 6.7 Ma (Figs. 3, 4 and 7). Although minima are comparable to values before 6.7 Ma, maxima in BFAR and organic matter content are up to six times higher after this time. After 5.8 Ma, echinoids increase parallel to the BFAR and support the possibility of increasing export productivity during the latest Miocene. Between 5.8 Ma and 5.25 Ma, the appearance of radiolaria points to a further increase in productivity or perhaps to a temporary intrusion of silica-rich water masses (Lange and Berger, 1993; Lange et al., 1999).

Can these fluctuations in productivity be related to changes in global ice volume? The large amplitude changes in productivity, especially the increase at 6.7–6.5 Ma and the four maxima, are not mirrored by changes in benthic foraminiferal $\delta^{18}O$ values (Fig. 9). Instead, a complicated pattern emerges. As an illustration, we compare $\delta^{18}O$ values, BFAR, and radiolarian accumulation rates against sample depths, which expands the data so that relations are more readily apparent in the low LSR intervals (Fig. 9). During two cold intervals, proxies for productivity (BFAR and TOC) have coeval minima (encircled on Fig. 9). However, apart from these two intervals, $\delta^{18}O$ changes generally correspond positively to BFAR variations, so that highest export paleoproductivity occurs in colder times (nos. 1–10 in Fig. 9) and lower productivity is in warmer intervals. Despite agreement between the timing of short-term variations in the proxies, the long-

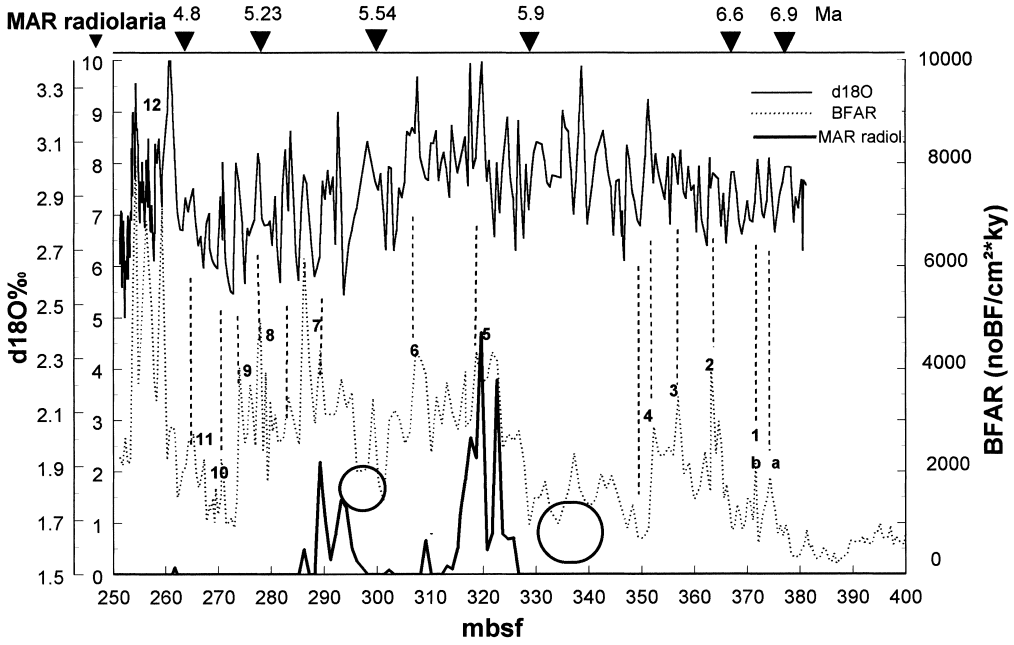

Fig. 9. Benthic foraminiferal $\delta^{18}O$ values, accumulation rates of benthic foraminifers (BFAR) (in numbers per cm^2/kyr), and accumulation rates of radiolarians (in mg/cm^2/kyr) versus depth in m below sea floor (mbsf) in sediments from ODP Site 1085 and biostratigraphic datum points in Ma. Circles mark intervals where $\delta^{18}O$ maxima correspond to BFAR minima. Numbers 1–12 refer to intervals where $\delta^{18}O$ maxima correspond to BFAR maxima and identify intervals where highest productivity occurs during cooler periods.

term trends do not correlate. For example, the trend in the BFAR is to increase upcore, whereas that of the $\delta^{18}O$ is to decrease from about 5.7 until 4.8 Ma and then to increase after 4.8 Ma. Moreover, radiolarian peak occurrences are in warmer intervals (Fig. 2, upper panel, Figs. 5 and 9), except for one radiolarian spike at 320 mbsf that is in a cold period.

The concordant increases in BFAR and $\delta^{18}O$ values imply a related origin. The maxima in BFAR (at 6.7–6.4, 5.7, 5.3–5.1, and 4.8 Ma) and in the TOC MAR (at 5.6, 5.3–5.1, and 4.8 Ma) (Fig. 4, upper panel and Fig. 7, upper panel) are in cooler periods (compare to Fig. 2, upper panel) when sea level was lower by some 30–40 m (Haq et al., 1987; Aharon et al., 1993; Vidal et al., 2002). Thus, it is possible that redeposited benthic foram shells reached Site 1085 by downslope transport from the shelf during lowstands (Diester-Haass, 1976, Summerhayes et al., 1995). In this case, changes in BFAR would reflect transport rather than productivity in the photic zone directly above Site 1085. This possibility is supported by the appearance of glauconite grains at Site 1085 during several of the cooler late Miocene periods (Fig. 8, upper panel). Grain-size analysis of benthic foraminifers confirms the occurrence of allochthonous benthic foraminifers in two intervals: between 4.85 and 4.7 Ma and between 5.6 and 5.5 Ma: 125–250 μm sized foraminifers increase whereas coarser ones decrease. These two intervals may consequently record periods of downslope supply of benthic forams together with glauconite and clastic particles, which are both enriched here and show an increase in sand (>63 μm)-sized particles (Fig. 8) and point to a regression and increased transport energy. However, an alternate explanation for the increase in smaller benthic foraminifers might be pulses in delivery of organic matter that enabled growth of smaller species, the 'phyto-detritus taxa', which carry most of the productivity signal in seasonal upwelling areas (Thomas et al., 1995; Gooday and Rathburn, 1999).

A similar correspondence between productivity variations as deduced from BFAR and glacial–interglacial cycles has been observed in late Quaternary sediments elsewhere in the Cape Basin (Schmiedl and Mackensen, 1997). At 3000 m water depth, interglacial values are about 200 BF/cm^2/kyr and increase up to 2800 BF/cm^2/kyr in glacial maxima. These values are lower than those we find at Site 1085 because of the greater water depth (3000 m vs. 1700 m) and because Schmiedl and Mackensen (1997) studied >150 μm foraminifers whereas we investigated the >125 μm fraction. Nonetheless, the magnitudes of the variations and the increases in glacial periods by a factor of 10 or more are comparable at the different locations and times.

The increase in export productivity that is reflected in BFAR during colder periods in the late Miocene as well as in the late Quaternary is probably a consequence of stronger winds and related stronger upwelling or vertical mixing in the surface ocean. These productivity maxima in colder periods are related to very low terrigenous input as reflected in highest $CaCO_3$ contents and lowest terrigenous matter in the coarse fraction and minima in magnetic susceptibility (Vidal et al., 2002; Wefer et al., 1998). During warmer periods, terrigenous supply was considerably higher. Following interpretations of Pliocene records by Sancetta et al. (1992), perhaps summer rainfall occurred during late Miocene interglacials and summer aridity occurred during late Miocene glacials in southwest Africa. Preliminary analyses of clay minerals in the <40 μm fractions of our samples support this scenario (Paturel, 2000). These analyses document an increase in smectite/illite ratios in warmer intervals that may reflect an increase in the Orange River discharge, which supplies mainly smectite (Bornhold, 1973; Diester-Haass et al., 1990), whereas higher illite contents during glacial periods indicate a relative increase in minerals delivered by wind from arid Namib areas (Diester-Haass et al., 1990).

Our interpretation of the late Miocene onset of productivity at Site 1085 is based mainly on BFAR and TOC and differs from the productivity history suggested by the opal contents, not only at Site 1085 but also at Site 362/532 on the Walvis Ridge (Fig. 1). The record of opal, if taken as a proxy for productivity, suggests that higher productivity is linked to warmer, interglacial periods on the Walvis Ridge since 5.4 Ma (using the time scale of Berggren et al., 1995) and late Pliocene (Diester-Haass et al., 1992; Sancetta et al., 1992). This discrepancy may result from the occurrence of opal in sediments under the Benguela Current actually serving as a recorder of silica availability in intermediate water masses rather than as a proxy of export productivity in this coccolithopore-dominated system (Lange and Berger, 1993; Lange et al., 1999).

Elevated productivity in surface waters can lead to increased dissolution of calcite on the underlying seafloor (Archer and Maier-Reimer, 1994) and thus to loss of $CaCO_3$ as long as oxygen content is high enough to allow benthic and bacterial life. However, our dissolution proxies – the B/P ratio and fragmentation of planktic foraminifers – do not reveal changes that are significantly related to productivity changes as inferred from BFAR and TOC. Also, $CaCO_3$ concentrations do not appear to be markedly diminished by dissolution. It seems that the $CaCO_3$ concentration is much more controlled by terrigenous dilution, in as much as most of the periods with high $CaCO_3$ concentrations are those with minima in terrigenous inputs (Fig. 8), and these periods generally correspond to cooler intervals. One important exception is the depression in $CaCO_3$ concentration at 6.5 Ma during a cold period. This period is related to medium magnetic susceptibility values, a rather low terrigenous input in the coarse fraction, and to low productivity. This event is the last of several $CaCO_3$ depressions during the late Miocene, and we attribute these low concentrations not to local changes in terrigenous input and productivity, but rather to the global middle to late Miocene 'carbonate crash' (Lyle et al., 1995; Pisias et al., 1995; Roth et al., 1999; Diester-Haass et al., 2001).

5.2. Broader implications

Our multiple productivity proxies at ODP Site 1085 indicate that the late Miocene was characterized by relatively low productivity until about

6.7–6.5 Ma, when a stepwise and highly variable increase in productivity began. This result is broadly similar to previous conclusions based on work done at DSDP sites on the Walvis Ridge (Siesser, 1980; Meyers et al., 1983). This late Miocene succession of events can be interpreted in terms of both local and global paleoceanographic changes.

Local changes in the Benguela Current upwelling system include an onset of upwelling over Site 1085 in the Cape Basin, a shift of existing upwelling cells westward (Siesser and Dingle, 1981), a seaward shift of the upwelling axis due to sea level regression, or a change in the intermediate water masses that provide nutrients to the upwelled water (Hay and Brock, 1991). The discrepancy between the productivity signal as established from BFAR and TOC on one hand and opal on the other hand points to the importance of the chemistry of upwelled water masses. Productivity maxima prior and subsequent to the radiolarian occurrences between 5.8 and 5.25 Ma do not contain opal. Radiolaria are a common element of modern shelf edge upwelling (Summerhayes et al., 1995), and the radiolarian spike we find might point to formerly stronger upwelling. The silica concentration of the upwelled water is an essential factor that controls the productivity, silica production, and preservation of radiolaria and diatoms (Lange and Berger, 1993; Lange et al., 1999). Hence it is possible that our radiolarian spike records greater availability of silica and consequently is not a simple proxy for upwelling strength.

If silica was more available between 5.8 and 5.25 Ma, then what was its source to the upwelled water masses? Hay and Brock (1992) suggest Antarctic intermediate water, and Berger et al. (1998) believe that the main silica source was the Angola Dome, which today supplies silica-rich and oxygen-depleted water to the southwest Africa margin in a southward undercurrent (Hart and Currie, 1960) that flows at 200–300 m water depth. We imagine that this poleward flowing current, which compensates for the upwelled water, became strong at about 5.8 Ma when the intertropical convergence zone shifted south with growth of bipolar ice caps (Hay and Brock, 1992) and when the strengths of local winds and of the Benguela Current increased enough to produce significant upwelling. Thus, the appearance of radiolaria in the Site 1085 record might be interpreted as a first signal of 'thermocline fertility' (Berger et al., 1998), whereas the overall increase in export paleoproductivity beginning at 6.7–6.5 Ma might be a signal of increased physical mixing and upwelling controlled by the wind field (the southeast trade winds).

Other paleoceanographic records suggest that the late Miocene increase in productivity in the Cape Basin is part of a global pattern. Increases in LSR and productivity similar to those at Site 1085 appear in the equatorial Pacific Ocean (Van Andel et al., 1975; Berger et al., 1993; Farrell et al., 1995), the equatorial Indian Ocean (Peterson et al., 1992; Dickens and Owen, 1999), the northwest Pacific Ocean (Rea et al., 1995), and the subpolar South Atlantic Ocean (Froelich et al., 1991). For example, in the equatorial Pacific Ocean LSRs increase by a factor of 5 and more between 7 and 6 Ma. These increases in LSRs correspond to dramatic increases in productivity proxies such as MARs of opal, carbonate, phosphorus, and barium (e.g. Van Andel et al., 1975; Schroeder et al., 1997). Furthermore, the same well-developed temporal variability in productivity during the high productivity interval present at Site 1085 also appears at equatorial Pacific locations (Schroeder et al., 1997; Farrell et al., 1995) and at ODP Site 704 on the Meteor Rise (Froelich et al., 1991). The productivity increase at Site 1085 begins at 6.7–6.5 Ma, and the time given by Farrell et al. (1995) for the onset of the biogenic bloom in the equatorial East Pacific is 7–6 Ma based on Shackleton et al. (1995), which corresponds to 6.7 Ma after Berggren et al. (1995). The shift to higher productivity at Site 704 is at 6.9 Ma (Froelich et al., 1991), after adjusting to the timescale of Berggren et al. (1995).

The productivity increase in the latest Miocene (6.9–6.5 Ma) at widespread locations raises several questions as to possible reasons: (1) Is the rather sudden increase in marine productivity the consequence of redistribution of nutrients within the oceans? (2) Was there an increase in supply of nutrients to the oceans? (3) Is there a

cause and effect relation between the middle/late Miocene 'carbonate crash' (Lyle et al., 1995) and the biogenic bloom?

Two mechanisms that could have redistributed nutrients within ocean basins are gradual shoaling of the Isthmus of Panama (Farrell et al., 1995, and references therein) and onset of NADW formation (Berger et al., 1993; Wright et al., 1991). However, Farrell et al. (1995) did not find a temporal link between the history of NADW and the onset of the biogenic bloom. Potential effects of the Messinian salinity crisis (Hodell et al., 1994, which after new dating by Krijgsman et al. (1999) at 5.96 Ma is too late to have contributed to the onset of the biogenic bloom) on the redistribution of nutrients within ocean basins is not yet understood.

The growth of the West Antarctic ice sheets (Shackleton and Kennett, 1975; Hodell et al., 1994 and references therein) and the initial growth of northern hemisphere ice caps since 7 Ma (Larsen et al., 1994) may have affected vertical nutrient distribution by increasing the equator to pole temperature gradient and thus intensifying atmospheric and oceanic circulation and therefore mixing in the ocean. The same mechanism has been attributed to the sudden rise in marine biological productivity in the earliest Oligocene during the substantial growth of Antarctic ice sheets (Diester-Haass and Zahn, 1996).

Another candidate to explain the latest Miocene biogenic bloom is enhanced flux of dissolved nutrients to the oceans (Dickens and Owen, 1999). The onset of Indian Ocean monsoons at 7–6 Ma (Molnar et al., 1993), a time that has been substantiated by climate modeling (Prell and Kutzbach, 1992), may have led to increased chemical weathering of continents and fluvial fluxes to the oceans. Increased delivery of Ca and Si and other nutrients necessary for increased production of carbonate and opaline fossils as observed in the latest Miocene may have been the consequence. A possible effect of monsoon circulation on wind systems in other parts of the world could be expected. Southeast trade winds may have intensified and contributed to the productivity increase between 6.7 and 6.5 Ma at Site 1085.

Our evidence of an export productivity increase at 6.7–6.5 Ma in the Cape Basin does not permit us to distinguish unequivocally between a local change in upwelling processes and thus onset of upwelling circulation off southwest Africa or to global changes in nutrient distribution or supply. We also cannot rule out a geochemical link between the middle/late Miocene 'carbonate crash' as observed in the Caribbean (Roth et al., 2000), the equatorial Pacific (Lyle et al., 1995; Berger et al., 1993) and the South Atlantic (Berger and Wefer, 1996; Diester-Haass et al., 2001), that ended about 300–600 kyr before the onset of high productivity (Diester-Haass et al., 2001). However, the coincident timing of similar increases in productivity at the many distant locations is striking, and it suggests the existence of a global connection of some kind.

6. Conclusions

We have reconstructed the late Miocene history of productivity at Site 1085 in the Cape Basin by means of accumulation rates of benthic foraminifera, total organic carbon, and radiolaria. Dramatic increases in BFAR and TOC MARs at 6.7–6.5 Ma record a sudden increase in export productivity. These proxies are also highly variable from 6.7 Ma to 4.8 Ma and indicate greater productivity in cooler intervals. Radiolaria occur only between 5.8 Ma and 5.25 Ma and suggest increased thermocline fertility mainly during warmer periods. Grain-size analyses of benthic foraminifers establish that BFAR maxima occurred during cooler periods and are not a consequence of downslope transport of foraminifers during sea level lowstands.

Terrigenous input seems to be the strongest factor that controls carbonate content and linear sedimentation rates. During cooler periods terrigenous input is smaller than during warmer times.

The sudden onset of high export productivity evident at Site 1085 at 6.7–6.5 Ma appears to be part of a global phenomenon. Similar increases between 6.9 Ma and 6.5 Ma are found in the equatorial and northeast Pacific and in the equatorial Indian Ocean. We conclude that the onset

of high export productivity in the Cape Basin is probably not simply a local signal of onset of upwelling but is part of a pattern of global paleoceanographic changes.

Acknowledgements

Stimulating discussions with Wolf Berger helped refine interpretations of our results. We thank Jerry Dickens for very helpful comments and suggestions that improved this manuscript. We thank Beth Christensen and Jacques Giraudeau for involving us in the Bordeaux meeting on Quaternary evolution of the Benguela coastal upwelling system, April 2000. P.A.M. thanks the Deep Sea Drilling Project and the Ocean Drilling Program, funded by the National Science Foundation and IPOD countries, for providing the unique opportunity to participate in both Leg 75 and Leg 175 and the Hanse-Wissenschaftskolleg, Delmenhorst, Germany, for its support during the preparation of this contribution. This study was supported by funds from the German Research Society and JOI-USSSP.

References

Archer, D., Maier-Reimer, E., 1994. Effect of deep-sea sedimentary calcite preservation on atmospheric CO2 concentration. Nature 367, 260–263.

Aharon, P., Goldstein, S.L., Wheeler, C.W., Jacobsen, G., 1993. Sea-level events in the South Pacific linked with the Messinian salinity crisis. Geology 21, 771–775.

Berger, W.H., 1989. Global maps of ocean productivity. In: Berger, W.H., Smetacek, V.S., Wefer, G. (Eds.), Productivity of the Ocean: Present and Past, Dahlem Conf. John Wiley, Chichester, pp. 429–455.

Berger, W.H., Leckie, R.M., Janecek, T.R., Stax, R., Takayama, T., 1993. Neogene carbonate sedimentation on Ontong Java Plateau: Highlights and open questions. In: Proc. ODP, Sci. Res. 130, 711–744.

Berger, W., Wefer, G., 1996. Expeditions into the past: paleoceanographic studies in the South Atlantic. In: Wefer, G., Berger, W.H., Siedler, G., Webb, D.J. (Eds.), The South Atlantic: Present and Past Circulation. Springer, Berlin, pp. 363–410.

Berger, W.H., Wefer, G., Richter, C., Lange, C.B., Giraudeau, J., Hermelin, O., Shipboard Scientific Party, 1998. The Angola-Benguela upwelling system: paleoceanographic synthesis of shipboard results from leg 175. In: Proc. ODP, Init. Rep. 175, 505–530.

Berggren, W.A., Kent, D.V., van Couvering, J.A. 1985. Neogene geochronology and chronostratigraphy. In: Snelling, N.J. (Ed.), The Chronology of the Geological Record. Mem. Geol. Soc. London 10, 211–260.

Berggren, W.A., Kent, D.V., Swisher, C.C., Aubry, M.-P., 1995. A revised Cenozoic geochronology and chronostratigraphy. SEPM, Spec. Publ. no. 54, 212 pp.

Bolli, H.M., Ryan, W.B.F. et al., 1978. Initial Reports of the Deep Sea Drilling Project vol. 40. US Government Printing Office, Washington, DC.

Bornhold, B.D., 1973. Late Quaternary sedimentation in the Eastern Angola Basin. Woods Hole Oceanogr. Inst. Tech. Rep. WHOI, pp. 773–778.

Cepek, M., Brückmann, W., Hay, W.W., Söding, E., Spiess, V., Thiede, J., Tiedemann, R., Wefer, G., 1999. Ocean Drilling Stratigraphic Network (ODSN), www.odsn.de. Integrated Chronostratigraphy for DSDP/ODP Drillsites in the South Atlantic Ocean.

Dickens, G.R., Owen, R.M., 1999. The latest Miocene-early Pliocene biogenic bloom: a revised Indian Ocean perspective. Mar. Geol. 161, 75–91.

Diester-Haass, L., 1976. Quaternary accumulation rates of biogenous and terrigenous components on the East Atlantic continental slope off NW Africa. Mar. Geol. 21, 1–24.

Diester-Haass, L., Zahn, R., 1996. The Eocene-Oligocene transition in the Southern Ocean: history of water masses, circulation, and biological productivity inferred from high resolution records of stable isotopes and benthic foraminiferal abundances (ODP Site 689). Geology 26, 163–166.

Diester-Haass, L., Meyers, P.A., Rothe, P., 1990. Miocene history of the Benguela Current and Antarctic ice volumes: evidence from rhythmic sedimentation and current growth across the Walvis Ridge (DSDP Sites 362 and 532). Paleoceanography 5, 685–707.

Diester-Haass, L., Meyers, P.A., Rothe, P., 1992. The Benguela Current and associated upwelling on the southwest African margin: a synthesis of the Neogene-Quaternary sedimentary record at DSDP sites 362 and 532. In: Summerhayes, C.P., Prell, W.L., Emeis, K.C. (Eds.), Upwelling Systems: Evolution since the Early Miocene. Geol. Soc. Lond. Spec. Publ. 64, 331–342.

Diester-Haass, L., Meyers, P.A., Vidal, L., Wefer, G., 2001. Data report: Sand fraction, carbonate, and organic carbon contents of Late Miocene sediments from Site 1085, middle Cape Basin. In: Proc. ODP, Sci. Res. 175, http://www.odp.tamu.edu/publications/175-SR/chap-01.

Farrell, J.W., Raffi, I., Janecek, T.R., Murray, D.W., Levitan, M., Dadey, K.A., Emeis, K.-C., Lyle, M., Flores, J.-A., Hovan, S., 1995. Late Neogene sedimentation patterns in the eastern equatorial Pacific. In: Proc. ODP, Sci. Res. 138, 717–756.

Froelich, P.N., Malone, P.N., Hodell, D.A. et al., 1991. Biogenic opal and carbonate accumulation rates in the subantarctic South Atlantic: the late Neogene of Meteor Rise Site 704. Proc. ODP, Sci. Res. 114, 515–550.

Gooday, A.J., Turley, C.M., 1990. Responses by benthic organisms to inputs of organic material to the ocean floor: a review. Philos. Trans. R. Soc. Lond. A 331, 119–138.

Gooday, A.J., Rathburn, A.E., 1999. Temporal variability in living deep-sea benthic foraminifera: a review. Earth Sci. Rev. 46, 187–212.

Haq, B.U., Hardenbol, J., Vail, P.R., 1987. Chronology of fluctuating sea level since the Triassic. Science 235, 1136–1167.

Hart, T.J., Currie, R.T., 1960. The Benguela Current. Discov. Rept. 31, 123–298.

Hay, W.W., Brock, J.C., 1992. Temporal variation in intensity of upwelling off southwest Africa. In: Summerhayes, C.P., Prell, W.L., Emeis, K.C. (Eds.), Upwelling Systems: Evolution since the Early Miocene. Geol. Soc. Lond. Spec. Publ. 64, 463–497.

Hay, W.W., Sibuet, J.-C. et al., 1984. Initial Reports of the Deep Sea Drilling Project vol. 75. US Government Printing Office, Washington, DC.

Herguera, J.C., Berger, W.A., 1991. Paleoproductivity from benthic foraminifera abundance: glacial to postglacial change in the west-equatorial Pacific. Geology 19, 1173–1176.

Hodell, D.A., Benson, R.H., Kent, D.V., Boersma, A., Racic-El Bied, K., 1994. Magnetostratigraphic, biostratigraphic, and stable isotope stratigraphy of an upper Miocene drill core from the Sale Briqueterie (Northwestern Morocco): A high resolution chronology for the Messinian stage. Paleoceanography 9, 835–855.

Krijgsman, W., Hilgen, F.J., Raffi, I., Sierro, F.J., Wilson, D.S., 1999. Chronology, causes and progression of the Messinian salinity crisis. Nature 400, 652–655.

Lange, C.B., Berger, W.H., 1993. Diatom productivity and preservation in the western equatorial Pacific: the Quaternary record. In: Berger, W.H., Kroenke, L.W., Mayer, L.A. et al. (Eds.), Proc. ODP, Sci. Res. 130, 509–523.

Lange, C.B., Berger, W.H., Lin, H.-L., Wefer, G., Shipboard Scientific Party Leg 175, 1999. The early Matuyama Diatom Maximum off SW Africa, Benguela Current System (ODP Leg 175). Mar. Geol. 161, 93–114.

Larsen, H.C., Saunders, A.D., Clift, P.D., Beget, J., Wei, W., Spezzaferi, S. et al., 1994. Seven million years of glaciation in Greenland. Science 264, 952–955.

Lutjeharms, J.R., Stockton, P.L., 1987. Kinematics of the upwelling of southern Africa. S. Afr. J. Mar. Sci. 5, 35–49.

Lyle, M., Dadey, K.A., Farrell, J.W., 1995. The late Miocene (11–8 MA) eastern Pacific carbonate crash: evidence for reorganisation of deep-water circulation by the closure of the Panama gateway. Proc. ODP, Sci. Res. 138, 821–838.

McRae, S.G., 1972. Glauconite. Earth Sci. Rev. 8, 397–440.

Meyers, P.A., Leg 75 Scientific Party, 1983. Organic geochemistry of Benguela Upwelling sediments recovered by DSDP/IPOD Leg 75. In: Thiede, J., Suess, E. (Eds.), Coastal Upwelling: Its Sediment Record (Part B). Plenum Press, New York, pp. 453–466.

Molnar, P., England, P., Martinod, J., 1993. Mantle dynamics, uplift of the Tibetian Plateau, and the Indian Monsoon. Rev. Geophys. 31, 357–396.

Müller, G., Gastner, M., 1971. The 'Karbonat-Bombe', a simple device for the determination of the carbonate content in sediments, soils and other materials. N. Jb. Mineral. 10, 466–469.

Nees, S., 1997. Late Quaternary palaeoceanography of the Tasman Sea: the benthic foraminiferal view. Palaeogeogr. Palaeoclimatol. Palaeoecol. 131, 365–389.

Nelson, D.M., Treguer, P., Brzezinski, M.A., Leynaert, A., Queguiner, B., 1995. Production and dissolution of biogenic silica in the ocean: revised global estimates, comparison with regional data and relationship to biogenic sedimentation. Glob. Biogeochem. Cycles 9, 359–372.

Paturel, J., 2000. Evolution des flux terrigenes dans le basin du Cap au Miocene superieur-Pliocene inferieur. Roles du systeme courantologique de Benguela et du climat africain. Mem. DEA, Univ. de la Mediterranee, Aix-Marseille II, 45 pp.

Peterson, L.C., Murray, D.W., Ehrmann, W.U., Hempel, P., 1992. Cenozoic carbonate accumulation and compensation depth changes in the Indian Ocean. In: Synthesis of Results from Scientific Drilling in the Indian Ocean. AGU Geophys. Monogr. 70, 311–333.

Pisias, N.G., Mayer, L.A., Mix, A.C., 1995. Paleoceanography of the eastern equatorial Pacific during the Neogene: Synthesis of Leg 138 Drilling results. Proc. ODP, Sci. Res. 138, 5–21.

Prell, W.L., Kutzbach, J.E., 1992. Sensitivity of the Indian monsoon to forcing parameters and implications for its evolution. Nature 360, 646–650.

Rea, D.K., Basov, I.A., Krissek, L.A., Leg 145 Scientific Party, 1995. Scientific results of drilling in the north Pacific transect. In: Proc. ODP, Sci. Res. 145, 577–596.

Roth, J.M., Droxler, A., Kameo, K., 2000. The Caribbean carbonate crash at the middle to late Miocene transition: linkage to the establishment of the modern global ocean conveyor. Proc. ODP, Sci. Res. 165, http://www.odp.tamu.edu/publications/165-SR/chap-17/.

Rogers, J., Bremner, J.M., 1991. The Benguela ecosystem, part VII. Marine Geological aspects. Oceanogr. Mar. Biol. Annu. Rev. 29, 1–85.

Sancetta, C., Heusser, L., Hall, M.A., 1992. Late Pliocene climate in the Southeast Atlantic: preliminary results from a multi-disciplinary study of DSDP Site 532. Mar. Micropaleontol. 20, 50–75.

Schmiedl, G., Mackensen, A., 1997. Late Quaternary paleoproductivity and deep water circulation in the eastern South Atlantic Ocean: evidence from benthic foraminifera. Paleogeogr. Paleoclimatol. Paleoecol. 130, 43–80.

Schroeder, J.O., Murray, R.W., Leinen, M., Pflaum, R.C., Janecek, T.R., 1997. Barium in equatorial Pacific carbonate sediment: terrigenous, oxide, and biogenic associations. Paleoceanography 12, 125–146.

Shackleton, N.J., Kennett, J.P., 1975. Late Cenozoic oxygen and carbon isotopic changes at DSDP Site 284: implications

for glacial history of the northern hemisphere and Antarctica. Init. Rep. Deep Sea Drill. Proj. 29, 801–807.

Shackleton, N.J., Crowhurst, S., Hagelberg, T., Pisias, N.G., Schneider, D.A., 1995. A new late Neogene time scale: application to Leg 138 sites. In: Proc. ODP, Sci. Res. 138, 73–101.

Shannon, L.V., Pillar, S.C., 1986. The Benguela ecosystem. Part III. Plankton. Oceanogr. Mar. Biol. Annu. Rev. 24, 65–170.

Shannon, L.V., Nelson, G., 1996. The Benguela: large scale features and processes and system variability. In: Wefer, G., Berger, W.H., Siedler, G., Webb, D.J. (Eds.), The South Atlantic: Present and Past Circulation. Springer Verlag, Berlin, pp. 163–210.

Siesser, W.G., 1980. Late Miocene origin of the Benguela upwelling system off northern Namibia. Science 208, 283–285.

Siesser, W.G., Dingle, R.V., 1981. Tertiary sea-level movements around Southern Africa. J. Geol. 89, 83–96.

Stramma, L., Peterson, R.G., 1989. Geostrophic transport in the Benguela Current region. J. Phys. Oceanogr. 19, 1440–1448.

Summerhayes, C.P., Kroon, D., Rosell-Melé, A., Jordan, R.W., Schrader, H.-J., Hearn, R., Vilanueva, J., Grimalt, J.O., Eglington, G., 1995. Variability in the Benguela Current upwelling system over the past 70.000 years. Progr. Oceanogr. 35, 207–251.

Thomas, E., Booth, L., Maslin, M., Shackleton, N.J., 1995. Northeastern Atlantic benthic foraminifera during the last 45.000 years: Changes in productivity seen from the bottom up. Paleoceanography 3, 545–562.

Van Andel, T.H., Heath, R.G., Moore, Jr., T.C., 1975. Cenozoic history and paleoceanography of the central equatorial Pacific Ocean: a regional synthesis of Deep Sea Drilling Project data. Geol. Soc. Am. Mem. 143, 143 pp.

van der Zwaan, G.J., Duijnstee, I.A.P., den Bulk, M., Ernst, S.R., Jannink, N.T., Kouwenhoven, T.J., 1999. Benthic foraminifers: proxies or problems? A review of paleoecological concepts. Earth Sci. Rev. 46, 213–236.

Verardo, D.J., Froelich, P.N., McIntyre, A., 1990. Determination of organic carbon and nitrogen in marine sediments using the Carlo Erba NA 1500 analyzer. Deep Sea Res. 37, 157–165.

Vidal, L. Bickert, L.T., Wefer, G., Roehl, U., 2002. Late Miocene stable isotope stratigraphy of SE Atlantic ODP Site 1085: relation to Messinian events. Mar. Geol. 180.

Wefer, G., Berger, W.H., Richter, C., Shipboard Party, 1998. Proceedings of the Ocean Drilling Program Initial Reports 175, http://odp-sun3.tamu.edu/publications/prelim/175-prelim/.

Wright, J.D., Miller, K.G., Fairbanks, R.G., 1991. Evolution of modern deep-water circulation. Evidence from the late Miocene Southern Ocean. Paleoceanography 6, 275–290.